International Research Journal of Innovations in Engineering and Technology (IRJIET)

ISSN (online): 2581-3048
Volume 7, Issue 11, pp 671-683, November-2023
https://doi.org/10.47001/IRJIET/2023.711089

Numerical Study of Solar Panel Cooling Using Paraffin-40 Combined with Nanomaterials on Variable Heat Flux

[1]Susanto, [2]*Nazaruddin Sinaga, [3]Syaiful, [4]Aji Digdoyo

[1,2,3,4]Department of Mechanical Engineering, Faculty of Engineering, Diponegoro University, Jalan Prof. Soedarto, Tembalang, Semarang 50275, Central Java, Indonesia
Authors E-mail: [1]massanto@students.undip.ac.id, [2]*nsinaga19.undip@gmail.com

***Abstract* - Many studies are being conducted to determine the optimal cooling arrangement for solar panels. One of the main issues that persists is the cooling effect used to lower the temperature of PV cells. The issue with natural convection air cooling surrounding solar panels is that it is thought to need to be more efficient in absorbing heat. It is necessary to implement effective and efficient cooling techniques. Phase Change Material (PCM) can be used as a cooling agent; the material should be chosen based on its melting point. The choice of a PCM depends on the climate and the material's thermal properties. PCM will absorb more heat throughout the melting process due to its higher latent heat than other materials. Analyzing PCM applications with nano-material addition was investigated numerically with Ansys Fluent. Pure PCM and a combination of nanomaterials were used in the cooling setup. A novel NPCM blend was made using the nanomaterials SiO_2 and Al_2O_3. The mass fraction of the additional nanomaterial is 1%, 5%, and 10%, respectively. Viscous laminar and transient flow conditions were used as methods for this study. The aim of this study is to examine the impact of paraffin-40 combined with nanomaterials on PV cell temperature lowering. PV cell temperature is reduced to 85.98 ^oC by applying pure paraffin-40 cooling at a heat flux of 1000 W/m^2. When Al_2O_3 composition is added at 1%, 5%, and 10%, the PV cell temperature decreases to 59.20, 53.46, and 48.06 ^OC, respectively. PV cells' temperature with the addition of SiO2 at compositions of 60.95, 59.62, and 57.46 ^oC, respectively. Blended materials with NPCM work well for solar panel passive cooling. A higher mass concentration of nanomaterials added to the composition has a more significant cooling effect. When added as an extra nanomaterial to PCM, Al_2O_3 performs better at cooling than SiO_2.**

Keywords: Nanomaterial; Mass Concentration; Phase Change Material; Passive Cooling; PV cell temperature.

I. INTRODUCTION

Solar panels can produce different amounts of electricity. The two main variables that affect how much power is generated are the solar panel's area and radiation intensity. Radiation intensity varies widely; the daily average is 399 W/m^2, and the midday peak is 1068 W/m^2 [1]. At peak radiation, problems with increasing the solar panel temperature arise. Increasing the irradiation value would increase the residual heat absorbed by the solar panel material. For example, a 120 WP solar panel can only generate 98.3 watts of electricity when the panel temperature reaches 70 ^OC [2]. The loss of power generation due to heat is enormous, with a reduction reached in the range of 18%. Cooling is necessary to reduce the solar panel's temperature during irradiation. Passive, active, or a combination of both cooling technologies can be developed according to the operational characteristics of each solar panel.

Problems in natural convection airflow cooling around solar panels are considered ineffective due to the impact of heat absorption. Low airflow velocity and high ambient temperatures are the causes of poor natural cooling. During midday, the ambient temperature can rise to 37 ^oC. Residual heat from solar radiation and ambient temperature make the solar panel temperature reach 75 ^OC [3]. Passive cooling without additional configurations will progressively lower efficiency if used on solar panels with larger sizes. The residual heat absorbed by the solar panel material also increases with increasing panel dimensions. Implementing passive cooling with excellent heat absorption capability is urgently needed. Passive cooling with high heat absorption capability can be an alternative cooling technology solution for solar panels. The high latent heat of PCM can be used to store heat from solar panels or dissipate it into the environment [4].

The latent heat of PCM, which is greater than that of other materials, will absorb more heat during the melting process. Cooling solar panels using PCMs can reduce the temperature of the panels without consuming electricity. The power consumption of the cooling technology does not bury the power generation increase. PCM melting time can be selected according to the preferred cooling temperature. PCMs with different melting temperatures of 27, 34, and 41 ^oC were studied for their cooling effect on solar panels [5]. The

International Research Journal of Innovations in Engineering and Technology (IRJIET)

ISSN (online): 2581-3048

Volume 7, Issue 11, pp 671-683, November-2023

https://doi.org/10.47001/IRJIET/2023.711089

selection of the PCM is based on the maximum temperature of the respective reference panels of 41, 52, and 75 ^{o}C at 279, 514 and 820 W/m^2 irradiance. Each region has different climatic conditions and solar radiation intensity.

A study in the equatorial region obtained highly variable ambient temperatures ranging from 25 ^{O}C to 34 ^{O}C throughout the year. The cooling method applied to solar panels in the area uses floating panels on the surface of a reservoir with a capacity of 1 MW and a central inverter system [6]. This research was conducted to obtain solar panels with high efficiency throughout the day in areas with sufficiently hot climatic conditions [7]. A tropical climate with hot ambient temperature characteristics significantly impacts power generation. Implementing solar panel cooling is necessary to maintain the stability of electricity generation and increase efficiency. Alternative cooling was implemented using a phase change material (PCM) medium.

Phase Change Material (PCM) has the characteristics of being thermal as an absorber, energy storage, and, at the same time, a good energy release. It can regulate the temperature of the environment. The PCM melting and solidification process occurs with high enthalpy at a constant temperature [8]. Applied PCM in solar panel cooling provides the benefit of learning the cooling effect of the decrease in PV cell temperature. The use of PCM is also still constrained by the low thermal conductivity of the substances. Thermal characteristics must be improved with a combination of other materials with better properties. Thermal characteristics can be improved by adding nanomaterials to a new material called nanomaterial PCM (NPCM). The novelty proposed in this research applies PCM-based passive cooling with the addition of nanomaterials. The NPCM mixture is expected to have better thermal characteristics to absorb more heat from the PV cell. The heat absorbed is greater, so the PV cell temperature cools down.

II. METHODOLOGY

2.1 Theory of Solar PV Panel

Arrangements of solar cells assembled in series into a single solar panel unit are available in various sizes and vary in power. A photovoltaic cell or module's electrical generation depends on many factors. The spectrum of incident solar radiation, the orientation of the cell relative to the solar beam, the operating temperature of the resulting cell, and the electrical load affect the electricity generation [9]. The amount of radiation from the sun is partly converted into electrical energy, partly lost, and partly absorbed and stored by the solar panel material, which is the energy balance that occurs [10]. The energy balance received by solar panels for electrical energy generation can be calculated using equation (1).

$$Q_{solar} = Q_{elect} + Q_{lost} + Q_{stored} \quad (1)$$

Where is(Q_{solar})Overall solar energy received, (Q_{elect})Energy that is converted into electrical energy, (Q_{lost}) Heat lost to the environment,(Q_{stored}) Heat is stored as residual in the solar panel material. The overall solar energy received by the solar panel can be described in the equation (2).

$$Q_{solar} = G.A_{PV}.\Delta t \quad (2)$$

Where is(G) The value of solar radiation received,(A_{PV})The area of the solar panel used, and(Δt) Time duration of irradiation and electricity generation.When the panel receives radiation, that's when the energy conversion process takes place. The conversion is in the form of electricity, with heat absorbed by the material and lost to the environment. The solar radiation entering the solar panel is the input power, which can be calculated using equation (3). Effects of radiation received by solar cells result in the occurrence of holes and movement of electrons, generating electricity into output power calculated by the equation (4).Solar energy converted into electrical energy is the electrical power generated over a specific period, which can be calculated using the equation (5).

$$P_{In} = G.A_{PV} \quad (3)$$

$$P_{Out} = V_{OC}.I_{SC}.FF \quad (4)$$

$$Q_{elect} = V_{OC}.I_{SC}.FF.\Delta t \quad (5)$$

Where is(P_{In}) The panel receive power,(P_{Out}) Generated power, (V_{OC}) Open circuit voltage, where no current flows (I) = 0, (I_{SC}) Current when the circuit is open, where there is no voltage (V) = 0. (FF) Fill Factor is an estimate of internal losses [9], and can be calculated using the equation (6). Internal losses of the solar panel by the solar cell material, impact the efficiency of the solar panel(η). Electric power generation can be calculated using the equation (7).

$$FF = \frac{V_{max}.I_{max}}{V_{OC}.I_{SC}} \quad (6)$$

$$\eta = \frac{Pout}{Pin} \text{ x } 100\ \% \quad (7)$$

Solar cell generation efficiency based on material type varies widely from 7.1 to 25.6% [11]. Energy received by solar cells is only slightly converted into electrical energy according to the value of cell material efficiency that can be achieved. Such low energy conversion in solar panels is influenced by the material characteristics, environmental temperature, and residual heat stored in the cell material. Energy loss can be calculated using the equation (8).

International Research Journal of Innovations in Engineering and Technology (IRJIET)

ISSN (online): 2581-3048

Volume 7, Issue 11, pp 671-683, November-2023

https://doi.org/10.47001/IRJIET/2023.711089

$$Q_{lost} = G.A_{PV}.(1-\alpha\tau) + h_{ca}.A_{PV}(T_{PV} - T_{amb}).\Delta t \quad (8)$$

Where is(α) The fraction of solar radiation absorbed by the solar panel with values between 0.85 - 0.95, (τ) A fraction of the solar radiation transmitted by the solar panel with a value of 0.9 – 1. (T_{PV}) and (T_{amb}) Are the ambient temperature and the surface temperature of the solar panel, respectively, and(h_{ca}) The combined heat loss coefficient between convection and radiation which can be calculated using the equation (9).

$$h_{ca} = 5{,}7 + 3{,}8\,V_w \qquad If\ V_w < 5\ \frac{m}{s}$$

$$h_{ca} = 6{,}47 + (V_w)^{0{,}78} \quad If\ V_w > 5\ \frac{m}{s} \qquad (9)$$

Where is(V_w) The wind speed surrounding the solar panel. Based on the equation (1) Overall solar energy received by solar panels is not entirely converted into electrical energy. In addition to energy lost to the environment, energy is also stored by the solar panel material. Stored energy(Q_{stored}) can be calculated using the equation (10) and (11).

$$\backslash Q_{stored} = Q_{solar} - (Q_{elect} + Q_{lost}) \qquad (10)$$

$$Q_{stored} = m.c.\Delta t \qquad (11)$$

Where is(m) The mass of the solar panel, which is made of multiple layers of material, with specific gravity(ρ)that are different, symmetrical shape that can be calculated(v),so that the mass value$(m = \rho.v)$. (c)Is the specific heat of each material layer.

2.2 Preparation PCM-nanomaterials

A cooling alternative for solar panels is to use Phase Change Material (PCM) as thermal energy storage. Passive cooling using PCMs can be more effective and efficient because no electricity consumption is generated. Cooling aims to improve performance by lowering the temperature of the entire solar panel layer. PCM is classified in phase change processes such as solid to liquid, solid to gas, and liquid to gas. A large amount of heat can be absorbed by PCM by the high latent heat of the phase change. The characteristic of heat storage by PCM occurs where a large amount of latent heat can be absorbed and released during phase change. During the phase change process, the temperature of the PCM remains constant. Temperature increases after the phase change to liquid, which is affected by sensible heat. The overall heat of PCM is obtained from the latent and sensible heat[12].The amount of calories can be calculated using the equation (12).

$$Q_{PCM} = m[C_{sp}(T_m - T_i) + \alpha_m \Delta h_m + C_{lp}(T_f - T_i) \quad (12)$$

Where is(Q_{PCM}) The heat capacity of PCM, (m) mass of PCM, (C_{sp}) specific heat of PCM in the solid phase, (T_m)Melting Temperature , (T_i) Initial Temperature, (α_m) Constant, (Δh_m) The difference in latent heat of melting, (C_{lp}) specific heat of PCM in the liquid phase, and(T_f) temperature of the liquid phase.

Using PCM in thermal and energy storage applications has various problems, such as liquid processes during melting, phase separation, supercooling, and low heat transfer rates [13]. Enhancement of heat absorption performance based on PCMs can use material additives with high thermal conductivity and porous media, using finned tubes and encapsulated PCMs to expand the heat transfer surface [14]. Nanomaterials are an alternative additive for PCMs to improve their thermal characteristics. The composition of nanomaterial additions to PCM can be compared with a mass or volume fraction. Phase Change Material (PCM) and nanomaterials used in this study have thermal characteristics presented in Table 1 below.

Table 1: Thermal Properties PCM dan Nanomaterials

Materials	MT (°C)	H (J/kg)	TC (W/m.K)	Density (kg/m^3)	SH (J/kg.k)
PCM P - 40	38 - 42	170000	0.25	800	2300
Nano Al_2O_3	-	-	35	3700	880
Nano SiO_2	-	-	1.4	2220	745

Incorporating nanomaterials has become an engineering method to improve heat transfer efficiency. Study results show that using nanomaterials can increase the heat transfer rate [15]. High latent heat with no subsequent increase in temperature during the phase change process is the main characteristic of PCM. During the phase change, the residual heat from the PV cell is absorbed. Latent heat is the cause of the heat absorption. The use of PCMs is the most highly promising technique for thermal energy storage due to their high energy storage density and nearly constant working temperature [14].

The preparation process of the mixture between PCM and nanomaterials can be done through characterization. The characterization is carried out in a chemical laboratory by melting the PCM material to a certain temperature. Liquid PCM is then given nanomaterials with a mass- or volume-fraction composition. For the mixture to be homogeneous, it

International Research Journal of Innovations in Engineering and Technology (IRJIET)

ISSN (online): 2581-3048

Volume 7, Issue 11, pp 671-683, November-2023

https://doi.org/10.47001/IRJIET/2023.711089

must be stirred with a rotation of 720 RPM for 38 minutes [12]. Mixtures are cooled to room temperature, and then the value of their thermal properties can be measured in the laboratory. The PCM+ nanomaterial characterization results in a material with new thermal properties. The material can be applied to solar panel cooling experimentally. In a numerical study involving NPCM, the value of thermal properties can be calculated using several equations. Density, specific heat, thermal conductivity, and latent heat of NPCM can be calculated using the equations (13), (14), (15), and (16).

$$\rho_{NPCM} = \phi\,\rho_{nm} + (1 - \phi)\,\rho_{PCM} \quad (13)$$

$$C_{p_{NPCM}} = \phi\,C_{p_{nm}} + (1 - \phi)\,C_{p_{PCM}} \quad (14)$$

$$K_{NPCM} = \frac{2K_{PCM}(1-\phi) + K_{nm}(1+2\phi)}{K_{PCM}(2+\phi) + K_{nm}(1-\phi)} \quad (15)$$

$$L_{NEPCM} = L_{PCM}(1 - \phi) \quad (16)$$

Where is(ρ_{NPCM}) The density of the PCM nano-mixture (ρ_{nm}) The density of pure nanomaterials, (ρ_{PCM}) The density of pure PCM, ($C_{p_{NPCM}}$) The specific Heat of PCM nano blends, ($C_{p_{nm}}$) The specific Heatof pure nanomaterials, ($C_{p_{PCM}}$) The specific Heatof pure PCM, (K_{NPCM}) Thermal conductivity of PCM nano blends,(K_{PCM})Thermal conductivity of pure PCM, (K_{nm}) Thermal conductivity of pure nanomaterials, (L_{NEPCM}) Latent Heat of PCM nano blends, (L_{PCM}) Latent heat of Pure PCM, and (∅) Composition of the mass fraction of nano material added to the pure PCM. The results of the calculation of the mixture of PCM and nanomaterials produce nano material PCM (NPCM) with new thermal properties. The NEPCM mixture with the composition of Al_2O_3 and SiO_2 nanomaterials of 1%, 5%, and 10% respectively is presented in Table 2 below.

Table 2: Thermal Properties NPCM

Materials NPCM	MT (°C)	H (J/kg)	TC (W/m.K)	Density (kg/m^3)	SH (J/kg.k)
P40 Al_2O_3 1 %	38 - 42	168300	1.5	829	2285.8
P40 Al_2O_3 5 %	38 - 42	161500	1.6	945	2229
P40 Al_2O_3 10 %	38 - 42	153000	1.8	1090	2158
P40 SiO21 %	38 - 42	168300	1.3	814.2	2284.5
P40 SiO25 %	38 - 42	161500	1.3	871	2222.3
P40 SiO210 %	38 - 42	153000	1.4	942	2144.5

2.3 Numerical Simulation

Numerical simulation was used to solve the solar panel cooling problem. The simulation process was carried out using the ANSYS program. The numerical method was used to solve various experimental problems. Problems such as PCM leakage, unstable solar irradiation, and other environmental factors reduce the accuracy of data acquisition. Numerical simulation only requires a few supporting properties when research is conducted experimentally.

Modeling is a simplified research method. A program such as ANSYS software can perform numerical analysis or simulation of an event for fluid behavior or heat transfer[17].CFD solution is carried out computationally by solving and analyzing software. The fluid flow is modeled based on the law of conservation of energy and mass with the following explanation.

1. Transient Flow

Simulation is completed with a Transient Flow model, where the flow that occurs changes over time. The selection of the transient model recognizes that solar irradiation also changes every time.

2. Incompressible Flow

When the density (ρ) of the fluid is constant, the flow is regarded as incompressible, which means there is no change in the density value in the presence of flow. If the air velocity of the flow velocity is below 100 m/s, it falls into the category of incompressible flow[18]. Three-dimensional incompressible fluid flow is expressed in the following Equation (17).

$$\frac{\partial_\rho}{\partial_x} = 0;\ \frac{\partial_\rho}{\partial_y} = 0;\ \frac{\partial_\rho}{\partial_z} = 0 \quad (17)$$

3. The Continuity Equation

At steady flow, the amount of mass in the control volume is fixed and can be expressed as in Equation (18).These statements are relevant to the law of conservation of mass, which states that mass cannot be created and destroyed.

$$\frac{\partial_u}{\partial_x} + \frac{\partial_v}{\partial_y} = 0 \quad (18)$$

Where is (u) The vector of velocity in the x-direction, and (v) The vector of velocity in the y-direction.

International Research Journal of Innovations in Engineering and Technology (IRJIET)

ISSN (online): 2581-3048

Volume 7, Issue 11, pp 671-683, November-2023

https://doi.org/10.47001/IRJIET/2023.711089

4. Navier–Stokes Equation

In this study, the ANSYS Fluent program modeled the case of natural convection and heat transfer. The natural convection that occurs simulates the natural airflow that hits the solar panel. Heat transfer occurs when the solar panel receives solar radiation and flows through each layer of the solar panel until it reaches the PCM. This program can simulate the solar radiation acting on the solar panel by entering the heat flux value on the surface of the solar panel. In a constant state of viscous, incompressible, velocity flow, and density (ρ), the momentum is expressed by the equation (19), (20), and (21).

$$\rho\left(\frac{\partial_u}{\partial_t}+u\frac{\partial_u}{\partial_x}+v\frac{\partial_u}{\partial_y}+w\frac{\partial_u}{\partial_z}\right)=-\frac{\partial_\rho}{\partial_x}+v\left(\frac{\partial^2{}_u}{\partial_{x^2}}+\frac{\partial^2{}_u}{\partial_{y^2}}+\frac{\partial^2{}_u}{\partial_{z^2}}\right) \quad (19)$$

$$\rho\left(\frac{\partial_v}{\partial_t}+u\frac{\partial_v}{\partial_x}+v\frac{\partial_v}{\partial_y}+w\frac{\partial_v}{\partial_z}\right)=-\frac{\partial_\rho}{\partial_y}+v\left(\frac{\partial^2{}_v}{\partial_{x^2}}+\frac{\partial^2{}_v}{\partial_{y^2}}+\frac{\partial^2{}_v}{\partial_{z^2}}\right) \quad (20)$$

$$\rho\left(\frac{\partial_w}{\partial_t}+u\frac{\partial_w}{\partial_x}+v\frac{\partial_w}{\partial_y}+w\frac{\partial_w}{\partial_z}\right)=-\frac{\partial_\rho}{\partial_z}+v\left(\frac{\partial^2{}_w}{\partial_{x^2}}+\frac{\partial^2{}_w}{\partial_{y^2}}+\frac{\partial^2{}_w}{\partial_{z^2}}\right) \quad (21)$$

2.3.1 Model dan Meshing

Simulations began by creating an engineering model that was used as a reference. The model is made by following the geometry, layer model, dimensions, and materials according to real conditions. The model design refers to previous research[19][20][21]. Reference solar panel has an electrical efficiency of 12% at 1000 W/m^2 irradiance with a temperature of 25^{O}C. The geometry model was created using the design modeler application.

The geometry model was made as a reference solar panel without cooling configuration composed of several layers of different materials. The solar panel with added coolant is the reference solar panel plus a Phase Change Material (PCM) coolant layer case. The results of the geometry modeling are presented in Figure 1 below. The modeled solar panel constituents have different material properties and dimensions, as presented in Table 3.

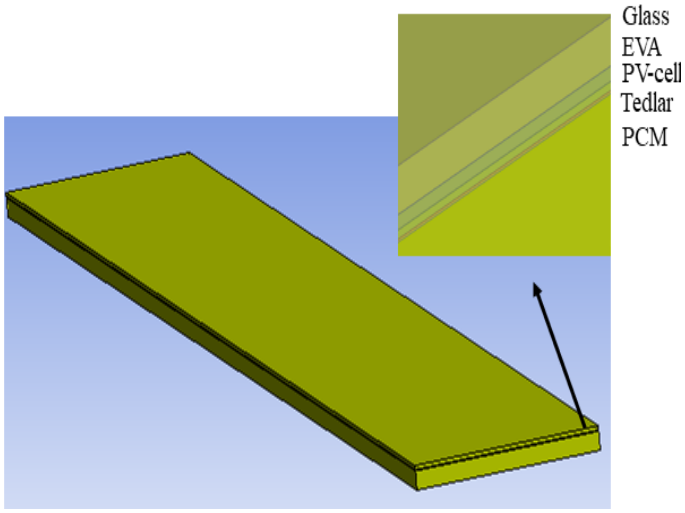

Figure 1: Model Solar Panel + PCM Layer

Table 3: Thermal Properties and Dimensions of Solar Panel + PCM Layer

Component	Density (kg/m^3)	TC (W/m.K)	SH (J/kg.k)	Dimensions(mm)
Glass cover	2200	0.76	830	1640 × 200 × 3.2
EVA layer	960	0.35	2090	1640 × 200 × 0.5
PV cells	2330	148	700	1640 × 200 × 0.3
Tedlar film	1200	0.20	1250	1640 × 200 × 0.1
PCM layer	As per applied PCM/NPCM			1640 × 200 × 15

Geometry modeled is then generated for meshing. The meshing process in each part of the domain is made into element cells of a certain size. Meshing was selected using the body sizing method. Scoping method using geometry selection. Each domain is selected, and the element size value is determined based on the dimensions of the solar panel model layer that is meshing. Skewness uses the default setup of 0.90000. Quality mesh is made with a smooth transition. Each surface layer and body domain is given a name to facilitate setting boundary conditions during the setup process. The meshing results of the geometry model created are presented in Figure 2.

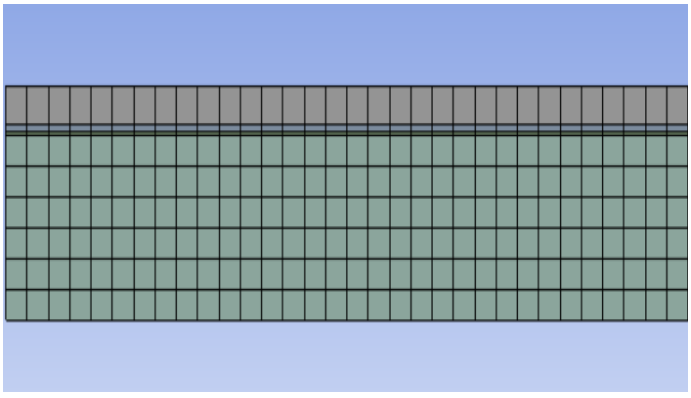

Figure 2: The Meshing Model

International Research Journal of Innovations in Engineering and Technology (IRJIET)
ISSN (online): 2581-3048
Volume 7, Issue 11, pp 671-683, November-2023
https://doi.org/10.47001/IRJIET/2023.711089

2.3.2 Set Up and Simulation Procedure

At the setup process, parameter values, material properties, and solver methods are determined to complete the calculations. The simulation uses a viscous laminar model, with energy on, which involves solidification and melting due to the PCM material used. The boundary condition setup for the simulation is guided by Figure 3.

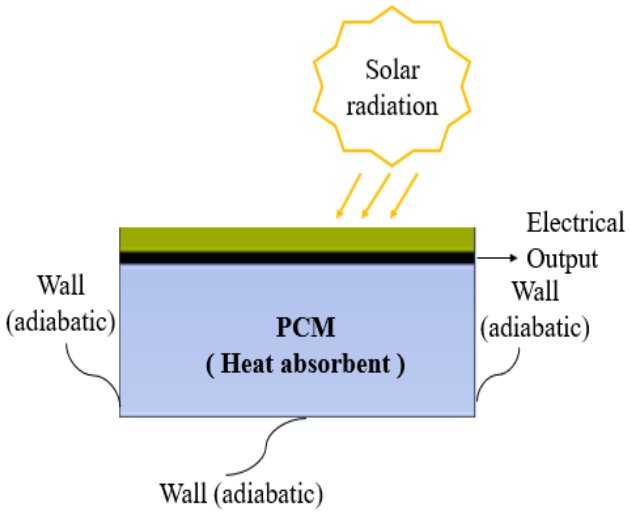

Figure 3: Boundary Condition

Figure 3 shows the boundary condition between the solar panel wall and PCM with the environment in the adiabatic wall state. Setting the adiabatic wall condition during simulation is done by entering the value of heat flux = 0, or convection wall[22].Solar radiation into the solar panel can be input as the heat flux value on the top layer of the glass surface. The heat flux values in this simulation are 50 W/m^2, 240 W/m^2, 540 W/m^2, 740 W/m^2, 940 W/m^2, and 1000 W/m^2. The simulation modeled air velocity and ambient temperature as 1 m/s and 30 ^{O}C, respectively. A pressure-based solution method was used to solve the problem. The SIMPLE algorithm was used with the PRESTO scheme to interpolate the pressure values at the surface. A second-order upwind scheme is used for spatial discretization.

III. RESULTS AND DISCUSSIONS

3.1 Result in Independent Grid Testand Validation

Computational Fluid Dynamic studies meshing produces a domain divided into many cells. Cell sizes vary, so the meshing process generates different elements. An independent grid test process needs to be performed to determine the number of cell elements for simulation. The PV-only model without cooling and the PV + PCM model were simulated for the independent grid test. Heat flux of 1000 W/m2was simulated for 1 hour for each cell element. The element cells created are 150000, 300000, 450000, 600000, 750000, and 900000. The grid test results and validation of the model are presented in Figure 4-7.

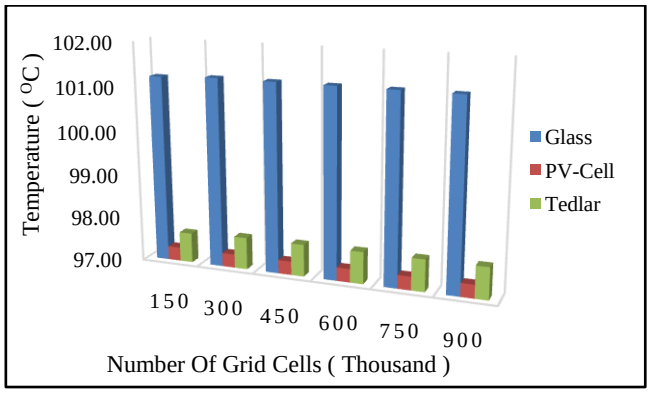

Figure 4: Grid Independent Test PV Only

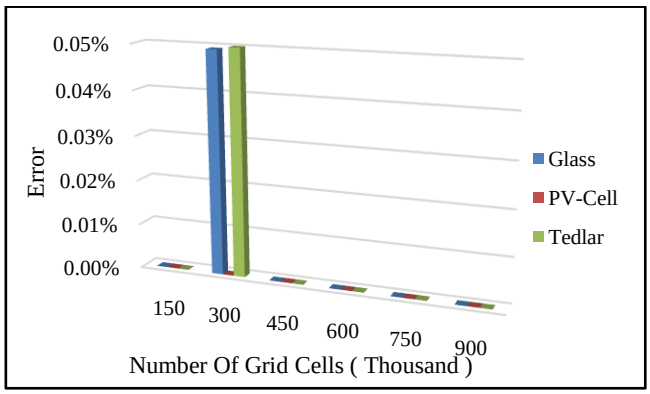

Figure 5: Error Grid Independent Test PV Only

Figure 4 above presents temperature data of Glass, PV Cell, and Tedlar. Temperature plot data is taken to calculate error and validation. The error between grids is calculated based on the temperature value of each number of cell elements. The error value is presented in Figure 5 above. The highest and lowest errors are 0.05% and 0.00% for the PV Only model.

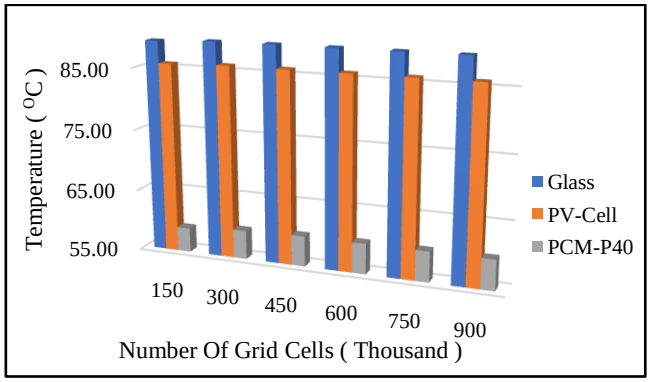

Figure 6: Grid Independent Test PV + PCM

International Research Journal of Innovations in Engineering and Technology (IRJIET)

ISSN (online): 2581-3048

Volume 7, Issue 11, pp 671-683, November-2023

https://doi.org/10.47001/IRJIET/2023.711089

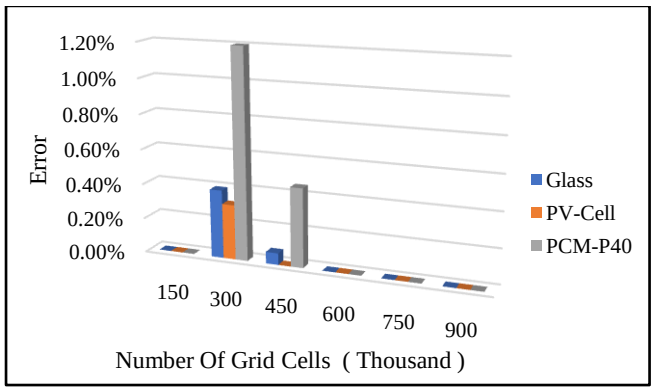

Figure 7: Error Grid Independent Test PV + PCM

Glass, PV Cell, and PCM temperatures were measured for the grid-independent test of the PV + PCM model presented in Figure 6 above. Figure 7 shows the error between grids calculated based on the measured temperatures. The highest grid error is 1.20%, and the lowest is 0%.

The highest error in the PV-only model is observed in the number of cell elements, 300000. The PV + PCM model has an error in the number of cell elements of 300000 and 600000. Depending on these results, the number of cell elements selected is 600000. Based on the results, the number of cell elements was decided to be 600000, considering that the error value is smaller and the number of cell elements is not too high. After the number of cells is determined, then validation is carried out.

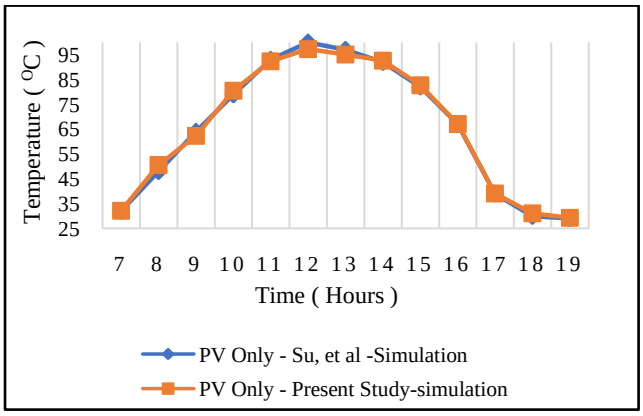

Figure 8: Temperature PV Cell Validation

Validation results are shown in Figure 8. Validation was performed on PV-only geometry without any cooling provided. Simulated PV cell temperature without PCM coolant is used as a reference for validation of the model made[20].The average temperature error from the model is 1.69%, with the lowest and highest errors of 0.32% and 5.33%.

3.2 Effect of Heat Flux on PV Cell Temperature

PV cells are part of solar panels that produce electrical power due to the flow of electrons. The power generated is strongly influenced by the radiation received, the area, and the PV cell's temperature when irradiating. Figures 9-16 present graphs of the effect of the heat flux value and the application of PCM paraffin-40 coolant as the base material. The PCM is also combined with nanomaterials in various mass fractions, and the cooling effect that can be achieved.

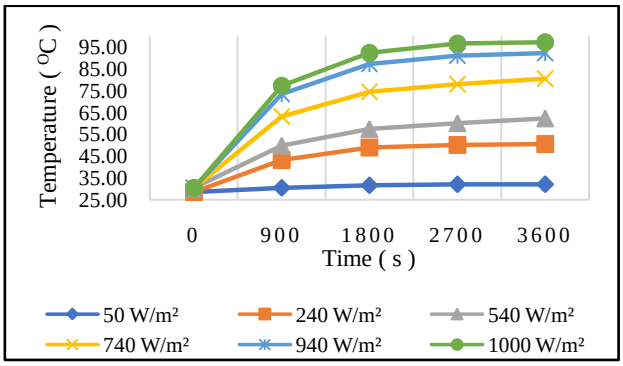

Figure 9: PV Cell Temp – PV Only

Results of the simulation of the PV-only model without cooling are presented in Figure 9. The model was simulated at various heat fluxes. Duration time is 3600 seconds for each given heat flux. The lowest and highest PV cell temperatures were 32.10 ^{O}C and 97.31 ^{O}C at heat fluxes of 50 W/m^2 and 1000 W/m^2, respectively. Each heat flux given gives the effect of different temperature values.

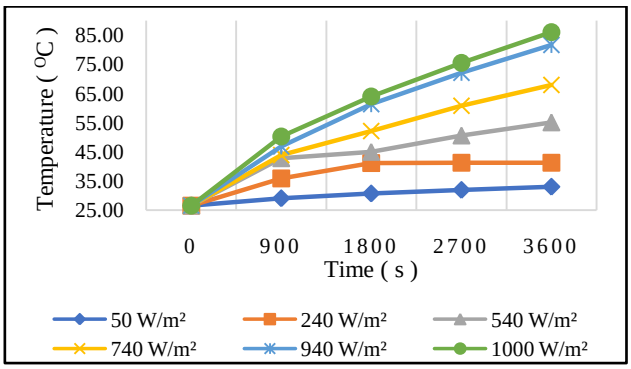

Figure 10: PV Cell Temp – PV + P40

Pure paraffin-40 PCM is employed for cooling simulations at various heat flux values. Figure 10 above presents the PV Cell temperature due to the given cooling effect of P40. At a heat flux of 1000 W/m^2, PV Cell temperature decreases to 85.98 ^{O}C and is the highest temperature. The cooling effect is also visible at lower heat flux from the lower PV Cell temperature compared to no cooling. At heat flux 50 W/m^2 and 240 W/m^2 PV Cell temperature at constant conditions below 41 ^{O}C.

International Research Journal of Innovations in Engineering and Technology (IRJIET)

ISSN (online): 2581-3048

Volume 7, Issue 11, pp 671-683, November-2023

https://doi.org/10.47001/IRJIET/2023.711089

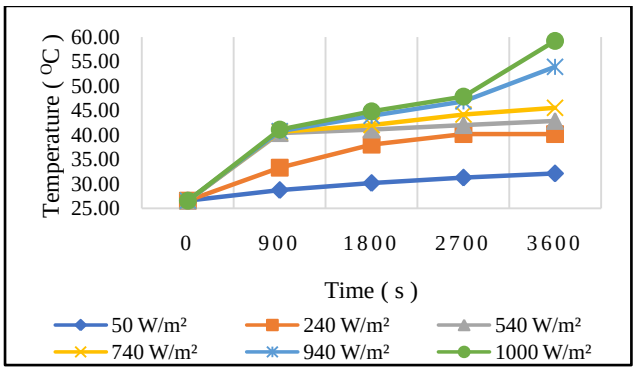

Figure 11: PV Cell Temp – PV + P40 + Al_2O_3 1 %

PV Cell temperature with a coolant mixture of NPCM P40 + Al_2O_3 1% produces a temperature graph in **Figure 11** above. PV Cell temperature is highest in the range of 59.20 ^OC at a heat flux of 1000 W/m^2. Adding Al_2O_3 1% mass fraction improves PV cell cooling temperature to 26 ^OC lower than PCM pure P40.

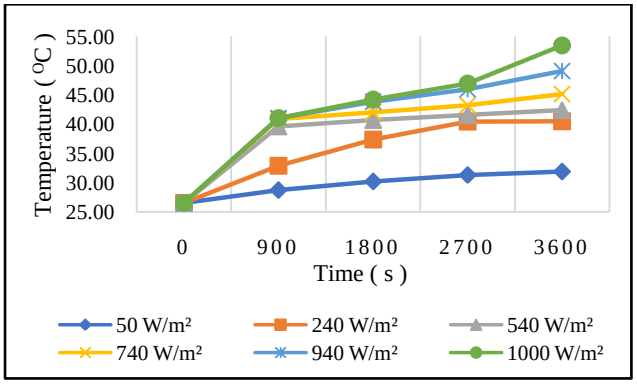

Figure 12: PV Cell Temp – PV + P40 + Al_2O_3 5 %

A mixture of NPCM P40 + 5% Al_2O_3 produces the graph in Figure 12 above. Adding 5% Al_2O_3 composition mass fraction further improves the cooling performance of the PV Cell—the PV Cell temperature at a heat flux of 1000 W/m^2 drops to 53.46 ^OC. The temperature is 6 ^OC lower than the 1% mixed composition. The temperature becomes lower at the same boundary condition.

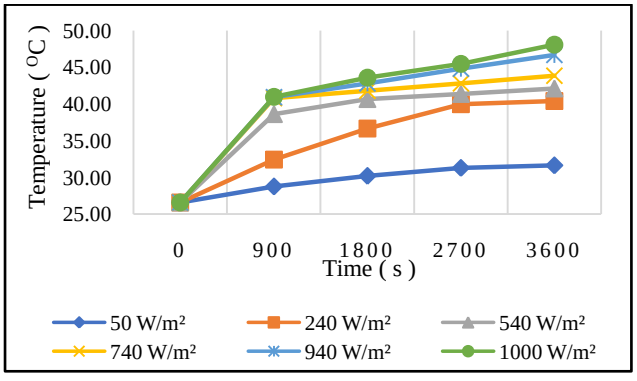

Figure 13: PV Cell Temp – PV + P40 + Al_2O_3 10 %

The cooling performance of the NPCM PV + P40 + Al_2O_3 10% mixture is the best. Based on the graph in Figure 13, the PV cell temperature drops 5 ^OC lower than the 5% composition at a heat flux of 1000 W/m^2. PV Cell temperature that can be achieved in the range of 48.06 ^OC.

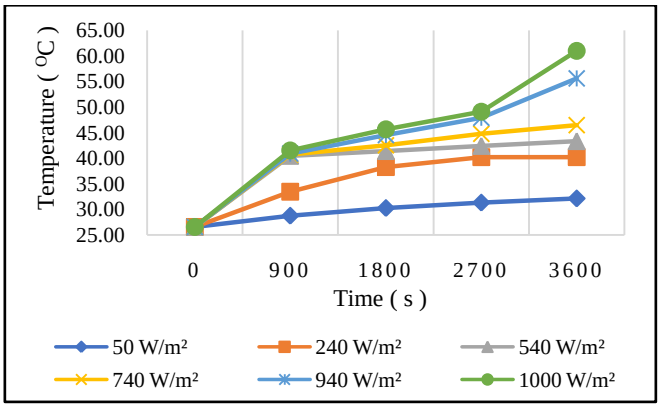

Figure 14: PV Cell Temp – PV + P40 + SiO_2 1 %

Different compositions using other materials make the blended material NPCM P40 + SiO_2 1%. The impact of cooling on PV cell temperature is presented in Figure 14 above. The PV cell temperature drops by about 25 to 60.95 ^OC compared to pure PCM at a heat flux of 1000 W/m^2.

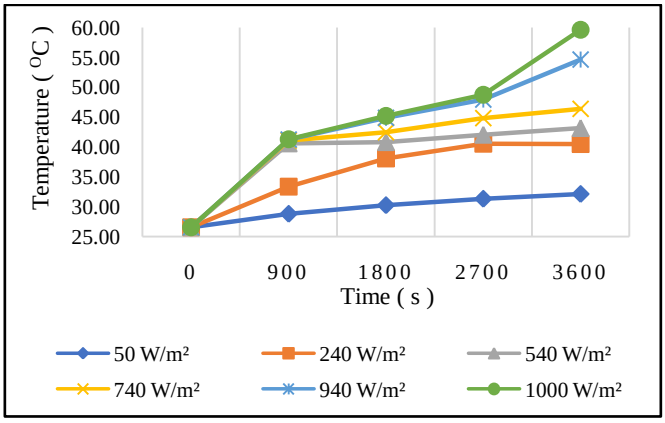

Figure 15: PV Cell Temp – PV + P40 + SiO_2 5 %

The composition of NPCM P40 + 5% SiO_2 has the cooling performance presented in Figure 15 above. Compared to the 1% composition, adding 5% SiO_2 has a less significant cooling impact. The decrease in PV Cell temperature at a heat flux of 1000 W/m^2 is only about 1.5 ^OC until the temperature drops to 59.62 ^OC.

International Research Journal of Innovations in Engineering and Technology (IRJIET)

ISSN (online): 2581-3048

Volume 7, Issue 11, pp 671-683, November-2023

https://doi.org/10.47001/IRJIET/2023.711089

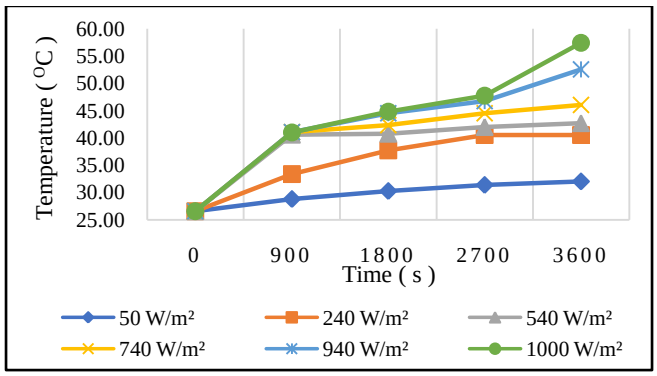

Figure 16: PV Cell Temp – PV + P40 + SiO_2 10 %

The temperature reduction effect of PV cell application of P40 + 10% SiO_2 mixed coolant is presented in **Figure 16** above. The 10% SiO_2 composition can reduce the PV cell temperature to 2 ^{O}C lower than the 5% mixture. At a heat flux of 1000 W/m^2, the temperature becomes 57.46 ^{O}C.

Analysis of each graph in Figures 9-16 shows that adding nanomaterial to paraffin-40 improves cooling. More mass concentration improves the heat absorption of the PV cell so that the temperature decreases. Nanomaterial of Al_2O_3 material has better cooling ability than SiO_2 material.

3.3 Effect of Heat Flux to PCM Temperature

The cooling process is a heat transfer process to reduce temperature. During the irradiation period, the cooling process also takes place. PCM material will absorb heat during phase change as a material that quickly changes phase. During phase change and melting, latent heat can absorb heat without increasing temperature. The increase in PCM temperature occurs when sensible heat works. Figures 17 - 23 present the temperature of PCM and NPCM during the simulation process at several heat fluxes.

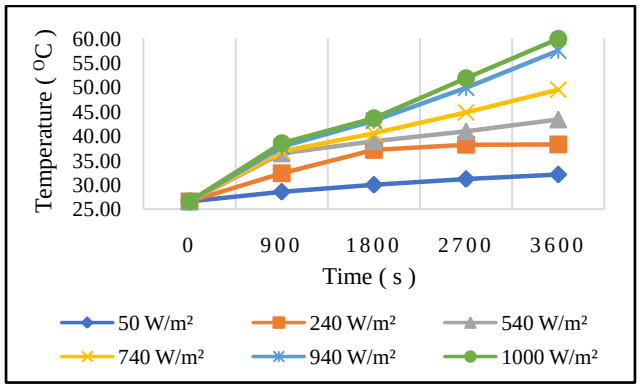

Figure 17: PCM Temp – P40 Pure

They used pure P40 as the cooling medium, increasing PCM temperature. The impact of temperature increase is presented in Figure 17 above. At a heat flux of 540 W/m^2, the PCM P40 temperature could stay at a melting temperature of 40 ^{O}C until 2700 seconds. At Heat flux 50 and 240 W/m^2 during irradiation 3600 seconds, there is no increase in temperature because the amount of heat entering cannot make PCM melt. At heat flux 1000 W/m^2, the PCM temperature continued to increase until 3600 seconds reached the highest temperature of 59.93 ^{O}C.

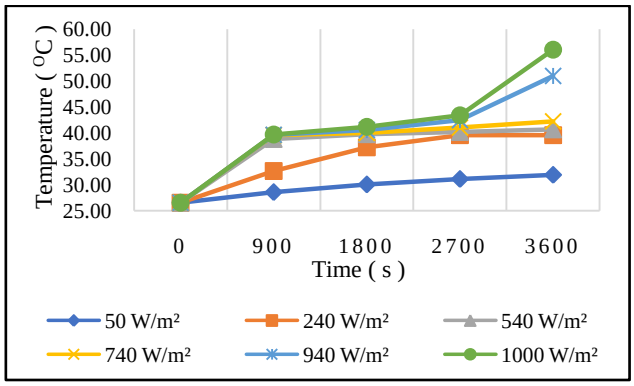

Figure 18: PCM Temp – P40 + Al_2O_3 1 %

A graphic of the temperature increase of NPCM P40 + Al_2O_3 1% is presented in Figure 18 above. At 1000 and 940 W/m^2 heat fluxes, the NPCM temperature can stay below 43 ^{O}C until 2700 seconds. After that, there was an increase in temperature because it was in the liquid phase and the influence of sensible heat so that it reached the highest temperature of 56.06 ^{O}C when the time reached 3600 seconds. At lower heat flux temperatures, NPCM does not increase in temperature significantly. NPCM can survive at low temperatures during phase change. This condition is because the phase change process has not ended.

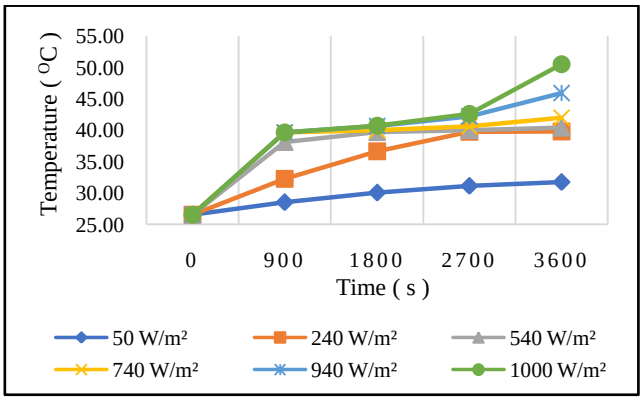

Figure 19: PCM Temp – P40 + Al_2O_3 5 %

Figure 19 above presents the NPCM P40 + 5% Al_2O_3 temperature increase graph. The trend of the NPCM temperature graph changes to be lower. At a heat flux of 1000 and 940 W/m^2, it can hold the NPCM temperature below 42 ^{O}C until the simulation time of 2700 seconds. The end of the phase change can be seen after the NPCM temperature has increased drastically due to the influence of sensible heat.

International Research Journal of Innovations in Engineering and Technology (IRJIET)

ISSN (online): 2581-3048

Volume 7, Issue 11, pp 671-683, November-2023

https://doi.org/10.47001/IRJIET/2023.711089

Until the simulation time reaches 3600 seconds, the highest temperature is in the range of 50.51 ^{O}C.

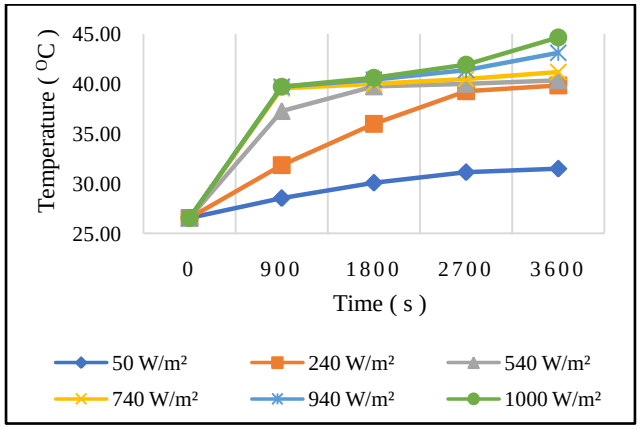

Figure 20: PCM Temp – P40 + Al_2O_3 10 %

Increasing the concentration of NPCM to P40 + Al_2O_3, 10%, can keep the NPCM at a low temperature for longer. Figure 20 above shows that the highest PCM temperature is in the range of 44.65 ^{O}C when a heat flux of 1000 W/m^2 is applied for 3600 seconds. When heat flux of 1000 and 940 W/m^2 is applied, the latent heat of NPCM can hold the PCM temperature at around 41 ^{O}C. The NPCM blend can provide a better heat transfer effect, with the cooling duration being longer.

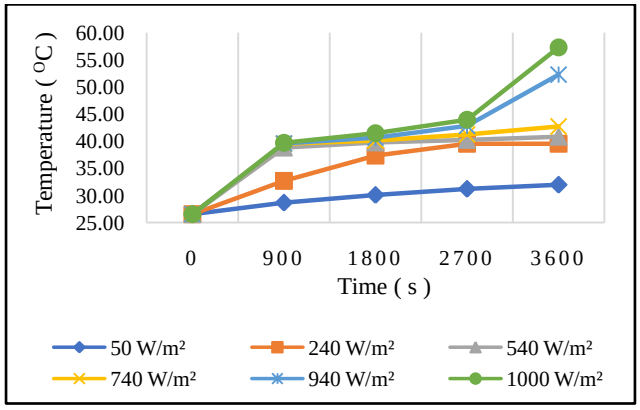

Figure 21: PCM Temp – P40 + SiO_2 1 %

Figure 21 above presents the graph of the temperature increase of NPCM with different nanomaterials. NPCM composition P40 + SiO_2 1% was used as the cooling agent. The mixture held the PCM temperature at 57.31 ^{O}C with a heat flux of 1000 W/m^2 for 3600 seconds. During the simulation time of 2700 seconds, the PCM temperature was below 43 ^{O}C.

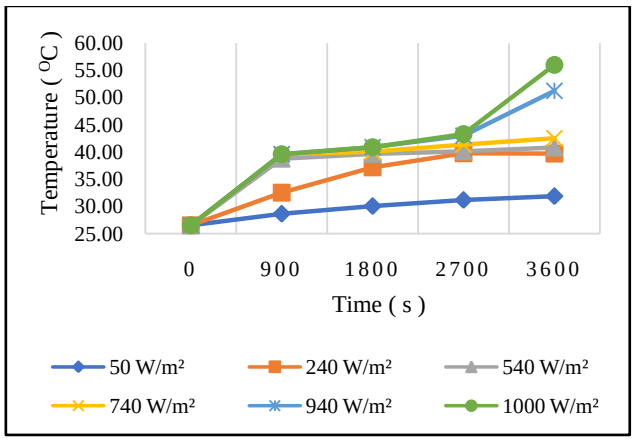

Figure 22: PCM Temp – P40 + SiO_2 5 %

The composition of the SiO_2 mixture was increased to produce NPCM P40 + SiO_2 5%. The NPCM temperature graph is presented in Figure 22 above. During the simulation of 2700 seconds with a heat flux of 1000 W/m^2, it could hold the NPCM temperature below 43 ^{O}C. The highest temperature is 56 or 1 ^{O}C lower than the 1% mixture composition.

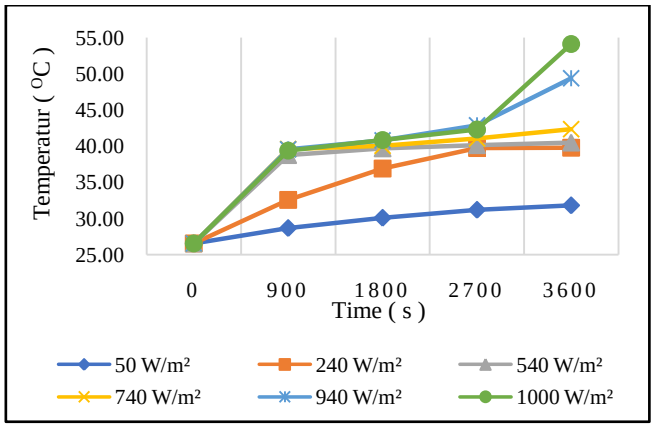

Figure 23: PCM Temp – P40 + SiO_2 10 %

Figure 23 presents the PCM temperature data with P40 + SiO_2 10% composition. The highest NPCM temperature with a heat flux of 1000 W/m^2 for a simulation duration of 3600 seconds is 54.12 ^{O}C. The temperature is 2 ^{O}C lower than the 5% composition. The NPCM temperature can stay below 42 ^{O}C at this heat flux for 2700 seconds.

Based on the analysis of each graph in Figures 17 - 23, adding nanomaterial has a better effect than pure PCM. Increasing the amount of nanomaterials mass composition in PCM has the impact of lowering the temperature of the mixture to be lower than the pure condition. Nanomaterials have better potential when applied to cooling solar panels with passive methods.

3.4 Temperature Contour

Visualisation of simulation results in contours can be used as a basis for analysis. The temperature of the simulated

International Research Journal of Innovations in Engineering and Technology (IRJIET)
ISSN (online): 2581-3048
Volume 7, Issue 11, pp 671-683, November-2023
https://doi.org/10.47001/IRJIET/2023.711089

model is displayed in the form of contour images with different colours. Based on the colour condition, the higher or lower temperature and the value of the temperature will be known. Figure 24 below presents the temperature contour of the solar panel with the application of pure paraffin PCM - 40-based coolant, with the NPCM provided with additional nanomaterial in various mass fractions.

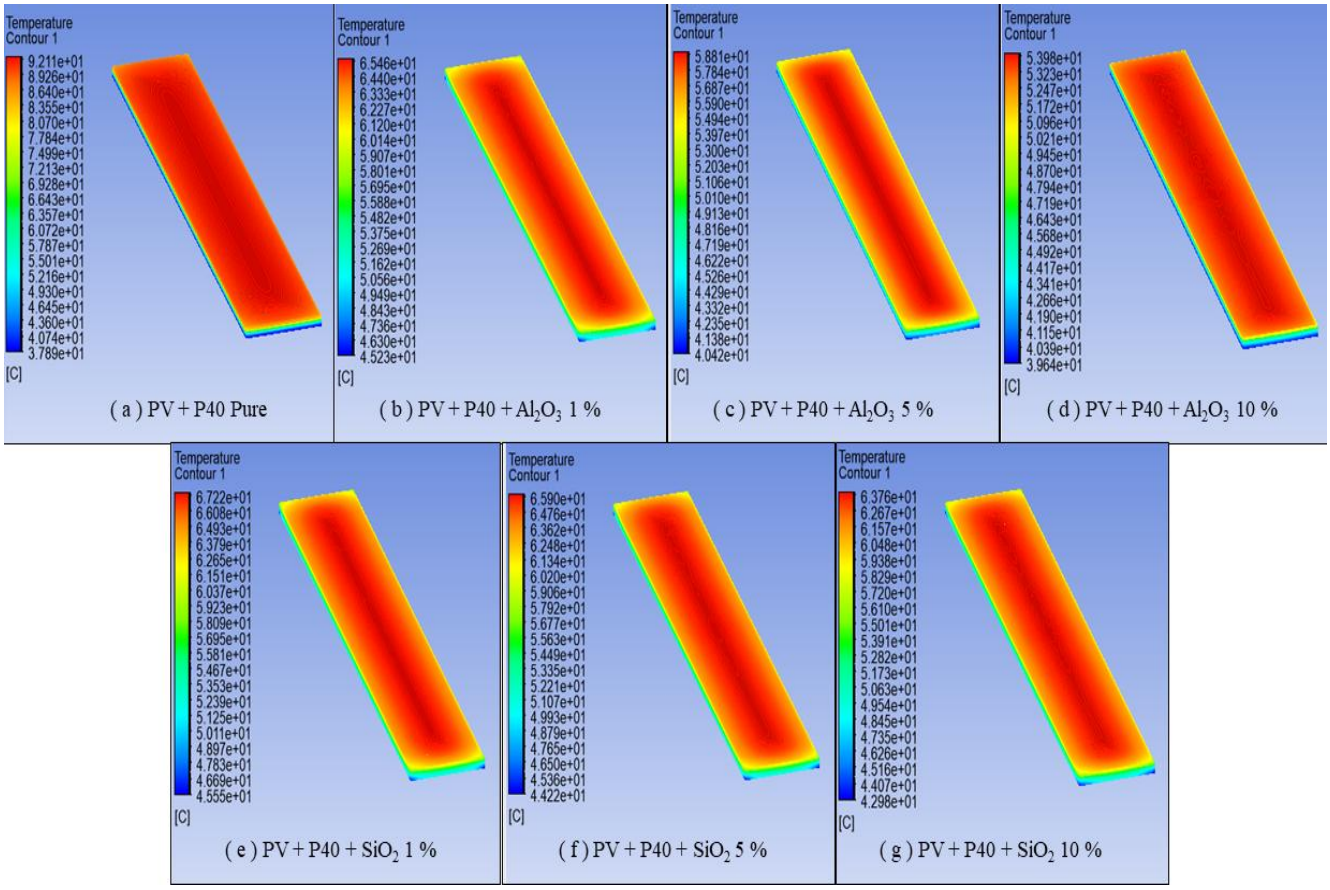

Figure 24: Static Temperature Contours with Cooling Paraffin - 40 + Nanomaterials

Figure 24 presents the temperature counts of solar panels with various cooling configurations with a heat flux of 1000 W/m^2. The effect of using PCM and NPCM can be seen from the color count; the temperature is highest on the top surface of the glass. More heat transfer occurs through the edges of the solar panel. This can be seen from the color gradation at the edges becoming lighter. This condition indicates that the PCM melting process is faster at the edges. The color in the middle of the glass layer looks darker, indicating that the temperature is higher than the edges.

IV. CONCLUSION

This article presents the results of a numerical study using Paraffin-40 with the addition of nanomaterials. This study helps to determine the ability of pure PCM and PCM with nanomaterial mixtures (NPCM) at several mass fraction concentrations. Based on the review of the simulation and analysis results, the following conclusions are obtained:

1) The value of heat flux received by the solar panel affects the temperature of the PV cell and the rise of PCM temperature during irradiation.
2) Pure paraffin-40 provides a good enough cooling effect so that the PV cell temperature drops by 12 ^{O}C compared to the PV cell without cooling.
3) Nanomaterial Al_2O_3 gives a better cooling effect, with a 1-2 ^{O}C lower temperature when compared with SiO_2 at the same mixture composition.
4) Adding nanomaterial mass compositions mixed in PCM can increase the thermal conductivity value and improve the cooling effect.

ACKNOWLEDGEMENT

The authors would like to acknowledge the Director of Politeknik Maritim Negeri Indonesia for providing permission for further study. The author would also like to acknowledge the Head of Efficiency and Energy Conservation Laboratory at Diponegoro University for his research support.

ISSN (online): 2581-3048
Volume 7, Issue 11, pp 671-683, November-2023
https://doi.org/10.47001/IRJIET/2023.711089

REFERENCES

[1] S. T. Mohammad, H. H. Al-Kayiem, M. A. Aurybi, and A. K. Khlief, "Measurement of global and direct normal solar energy radiation in Seri Iskandar and comparison with other cities of Malaysia," *Case Stud. Therm. Eng.*, vol. 18, no. October 2019, pp. 0–9, 2020, doi: 10.1016/j.csite.2020.100591.

[2] M. K. S. Al-Ghezi, R. T. Ahmed, and M. T. Chaichan, "The Influence of Temperature and Irradiance on Performance of the Photovoltaic Panel in the Middle of Iraq," *Int. J. Renew. Energy Dev.*, vol. 11, no. 2, pp. 501–513, 2022, doi: 10.14710/ijred.2022.43713.

[3] P. Manoj Kumar et al., "Investigating performance of solar photovoltaic using a nano phase change material," *Mater. Today Proc.*, vol. 47, no. xxxx, pp. 5029–5033, 2021, doi: 10.1016/j.matpr.2021.04.615.

[4] B. V. Rudra Murthy and V. Gumtapure, "Thermo-physical analysis of natural shellac wax as novel bio-phase change material for thermal energy storage applications," *J. Energy Storage*, vol. 29, no. March, 2020, doi: 10.1016/j.est.2020.101390.

[5] H. A. Refaey, M. H. Wahba, H. E. Abdelrahman, M. Moawad, and N. S. Berbish, "Experimental Study on the Performance Enhancement of the Photovoltaic Cells by Using Various Nano-Enhanced PCMs," *J. Inst. Eng. Ser. C*, vol. 102, no. 2, pp. 553–562, 2021, doi: 10.1007/s40032-020-00655-7.

[6] A.P. Sukarso and K. N. Kim, "Cooling effect on the floating solar PV: Performance and economic analysis on the case of west Java province in Indonesia," *Energies*, vol. 13, no. 9, 2020, doi: 10.3390/en13092126.

[7] D. A. Widodo, P. Purwanto, and H. Hermawan, "Modeling solar potential in semarang, indonesia using artificial neural networks," *J. Appl. Eng. Sci.*, vol. 19, no. 3, pp. 578–585, 2021, doi: 10.5937/jaes0-29025.

[8] C. Cercignani, "Phase Change Material And Their Basic Properties," *in Mathematical Methods in Kinetic Theory*, 2007, pp. 39–65. doi: 10.1007/978-1-4899-5409-1_2.

[9] B. H. Hamadani and B. Dougherty, "Solar cell characterization," *Semicond. Mater. Sol. Photovolt. Cells*, pp. 229–245, 2015, doi: 10.1007/978-3-319-20331-7_8.

[10] A.Hasan, S. J. McCormack, M. J. Huang, and B. Norton, "Energy and cost saving of a photovoltaic-phase change materials (PV-PCM) System through temperature regulation and performance enhancement of photovoltaics," *Energies*, vol. 7, no. 3, pp. 1318–1331, 2014, doi: 10.3390/en7031318.

[11] G. Martin A, K. Emery, Y. Hishikawa, W. Warta, and D. D., "Solar cell efficiency tables (Version 45)," *Prog. Photovoltaics Res. Appl.*, vol. 20, no. 1, pp. 6–11, 2015, doi: 10.1002/pip.

[12] P. Alam, N. K. Gupta, and A. R. Nizam, "Characterization of nanoparticles embedded phase change materials," *Mater. Today Proc.*, vol. 26, no. xxxx, pp. 2932–2937, 2019, doi: 10.1016/j.matpr.2020.02.606.

[13] W. Aftab, X. Huang, W. Wu, Z. Liang, A. Mahmood, and R. Zou, "Nanoconfined phase change materials for thermal energy applications," *Energy Environ. Sci.*, vol. 11, no. 6, pp. 1392–1424, 2018, doi: 10.1039/c7ee03587j.

[14] Y. B. Tao and Y. L. He, "A review of phase change material and performance enhancement method for latent heat storage system," *Renew. Sustain. Energy Rev.*, vol. 93, no. April, pp. 245–259, 2018, doi: 10.1016/j.rser.2018.05.028.

[15] M. Alhuyi Nazari et al., "A review of nanomaterial incorporated phase change materials for solar thermal energy storage," *Sol. Energy*, vol. 228, no. September 2020, pp. 725–743, 2021, doi: 10.1016/j.solener.2021.08.051.

[16] M. Sheikholeslami, "Numerical investigation for concentrated photovoltaic solar system in existence of paraffin equipped with MWCNT nanoparticles," *Sustain. Cities Soc.*, vol. 99, no. August, 2023, doi: 10.1016/j.scs.2023.104901.

[17] Z. Arifin, S. Suyitno, D. D. D. P. Tjahjana, W. E. Juwana, M. R. A. Putra, and A. R. Prabowo, "The effect of heat sink properties on solar cell cooling systems," *Appl. Sci.*, vol. 10, no. 21, pp. 1–16, 2020, doi: 10.3390/app10217919.

[18] J. H. Kim, S. H. Park, and J. T. Kim, "Experimental performance of a photovoltaic-thermal air collector," *Energy Procedia*, vol. 48, pp. 888–894, 2014, doi: 10.1016/j.egypro.2014.02.102.

[19] M. C. Browne, B. Norton, and S. J. McCormack, "Heat retention of a photovoltaic/thermal collector with PCM," *Sol. Energy*, vol. 133, pp. 533–548, 2016, doi: 10.1016/j.solener.2016.04.024.

[20] D. Su, Y. Jia, Y. Lin, and G. Fang, "Maximizing the energy output of a photovoltaic–thermal solar collector incorporating phase change materials," *Energy Build.*, vol. 153, pp. 382–391, 2017, doi: 10.1016/j.enbuild.2017.08.027.

[21] A.Salari, A. Kazemian, T. Ma, A. Hakkaki-Fard, and J. Peng, "Nanofluid based photovoltaic thermal systems integrated with phase change materials: Numerical simulation and thermodynamic analysis," *Energy Convers. Manag.*, vol. 205, no. June 2019, p. 112384, 2020, doi: 10.1016/j.enconman.2019.112384.

ISSN (online): 2581-3048
Volume 7, Issue 11, pp 671-683, November-2023
https://doi.org/10.47001/IRJIET/2023.711089

[22] S. Ahdy, M. A. Boraey, H. Abdel Hameed, and H. El Salmawy, "Effect of the wall thermal boundary condition on the structure of a confined swirling diffusion flame," *J. Brazilian Soc. Mech. Sci. Eng.*, vol. 41, no. 11, pp. 1–12, 2019, doi: 10.1007/s40430-019-2007-1.

Citation of this Article:

Susanto, Nazaruddin Sinaga, Syaiful, Aji Digdoyo, "Numerical Study of Solar Panel Cooling Using Paraffin-40 Combined with Nanomaterials on Variable Heat Flux" Published in *International Research Journal of Innovations in Engineering and Technology - IRJIET*, Volume 7, Issue 11, pp 671-683, November 2023. Article DOI https://doi.org/10.47001/IRJIET/2023.711089

****

